

Magnetic Dipole–Dipole Interactions and Single-Ion Anisotropy: Revisiting a Classical Approach to Magnets

C. M. Wynn, M. A. Girtu, and W. B. Brinckerhoff

Department of Physics, The Ohio State University, Columbus, Ohio 43210-1106

K.-I. Sugiura and Joel S. Miller

Department of Chemistry, University of Utah, Salt Lake City, Utah 84112

A. J. Epstein*

Department of Physics and Department of Chemistry, The Ohio State University, Columbus, Ohio 43210-1106

Received April 29, 1997. Revised Manuscript Received July 25, 1997[⊗]

The weak classical through-space magnetic dipolar interactions have, in general, not been an important component in stabilizing bulk magnets, as the strong quantum-mechanical through-bond exchange couplings dominate. We show that for materials composed of strongly exchange-coupled magnetic chains with very weak interchain exchange, the interchain dipolar interactions may dominate, leading to sizable ordering temperatures. The single-ion anisotropy together with the anisotropy of the dipole interaction determine the magnetic ordering directions. The family of [Mn(porphyrin)]⁺[cyanocarbon][−] magnets is shown to order due to classical interchain dipolar interaction in combination with the single-ion anisotropy, resulting in canted magnetic structures.

Introduction

Since the discovery of [Fe(C₅Me₃)₂][TCNE] (TCNE = tetracyanoethylene), the first molecule-based magnet with a spontaneous moment and magnetic hysteresis¹ (at 4.8 K), the development and exploration of molecule-based materials that exhibit bulk ferromagnetic properties at higher temperatures has been a focus of an ever-increasing amount of experimental research.² In contrast to conventional atom-based magnets such as iron or cobalt, molecule-based systems potentially offer the advantages of enhanced processability (many will dissolve in common solvents) and low density, in addition to biocompatibility. Furthermore, some materials may have optical properties (transparent at visible frequencies) useful in a variety of different technological applications.³

A bulk magnetic moment is a cumulative effect due to the coupling of unpaired electron spins throughout a solid. During the past decade, a variety of ingenious design strategies have been employed to create a spontaneous moment in a molecule-based system. These strategies, which focus on intersite interactions, may be divided into two categories based upon the two limiting types of interactions between neighboring spin-

carrying units: antiferromagnetic (AFM), in which antiparallel neighboring spins is the lower energy state, and ferromagnetic (FM), in which parallel neighboring spins is the lower energy state. In addition to the limiting parallel (FM) and antiparallel (AFM) spin orientation patterns, canted antiferromagnets occur when the neighboring spins are canted (no longer parallel or antiparallel) with each other. A canted AFM will have a net magnetic moment, though of reduced magnitude to that of a FM. While examples of FM interactions exist,⁴ FM coupling is significantly less prevalent in nature than AFM coupling and research on ferromagnetically coupled compounds remains challenging.⁵

Use of AFM interactions to generate a net moment may seem impossible; however, in the special case of a ferrimagnet a net moment indeed can occur. A ferrimagnet is a magnet in which two differing spins are aligned antiparallel (AFM) to one another. This spin inequivalency leads to an incomplete cancellation of the moments and, like a ferromagnet, a resulting net magnetization below an ordering temperature, *T_c*. An isolated linear chain (one-dimensional or 1D) system will not order (and thus not produce a net moment) above absolute zero.⁶ Ordering requires both intra- and interchain interactions; only when magnetic coupling between the chains exist can the system order. Several synthetic approaches have been exploited to achieve

[⊗] Abstract published in *Advance ACS Abstracts*, September 15, 1997.

(1) Miller, J. S.; Epstein, A. J.; Reiff, W. M. *Mol. Cryst. Liq. Cryst.* **1985**, *120*, 27. Chittipeddi, S.; Cromack, K. R.; Miller, J. S.; Epstein, A. J. *Phys. Rev. Lett.* **1987**, *58*, 2695. Miller, J. S.; Calabrese, J. C.; Rommelmann, H.; Chittipeddi, S.; Epstein, A. J.; Zhang, J. H.; Reiff, W. M. *J. Am. Chem. Soc.* **1987**, *109*, 769.

(2) For example see: *The Proceedings of the Fourth International Conference on Molecule-Based Magnets*, Miller J. S.; Epstein, A. J., Eds.; *Mol. Cryst. Liq. Cryst.* **1994**, 271–274.

(3) Landee, C. P.; Melville, D.; Miller, J. S. In *Magnetic Molecular Materials*; Gatteschi, D., Kahn, O., Miller, J. S., Palacio, F., Eds.; Kluwer Academic Publishers: Dordrecht, 1991; p 395. Miller, J. S. *Adv. Mater.* **1994**, *6*, 322.

(4) Tamura, M.; Nakazaw, Y.; Shiomi, D.; Nozawa, K.; Hosokoshi, Y.; Ishikaw, M.; Takahashi, M.; Kinoshita, M. *Chem Phys. Lett.* **1991**, *186*, 401. Miller, J. S.; Epstein, A. J.; Reiff, W. M. *Science* **1988**, *240*, 40.

(5) Carlin, R. L. *Comments Inorg. Chem.* **1991**, *11*, 215.

(6) de Jongh, L. J.; Miedema, A. R. *Experiments On Simple Magnetic Model Systems*; Taylor and Francis: London, 1974; p 28.

ferrimagnetic chains.^{7–9} The ordering in these systems indicates higher-dimensionality, i.e., interchain interactions. The control of these interactions is the major hurdle for most materials architectures. A systematic approach to the ferromagnetic coupling of these chains has been absent. Herein we discuss the importance of magnetic dipole interchain interactions and the single-ion anisotropy (SIA) in determining T_c and the type of parallel, canted, or antiparallel magnetic ordering.

Magnetic dipole interactions are a classical effect due to the magnetic field generated by a magnetic moment and this field's through-space effects on its neighbors. Most textbooks¹⁰ point out that while magnetic dipole interactions control the macroscopic movements of compass needles and iron filings, they are almost never responsible for the microscopic alignment of the spins that form bulk magnets. For a few materials, however, the dipolar interactions have been reported as responsible for the ordering. Studies¹¹ beginning in the 1960s indicated that many rare-earth-based compounds, such as EuSO_4 ,¹² order near 1 K due to dipolar interactions. In the 1970s, studies of the TMMC family indicated a three-dimensional AFM ground state near 1 K likely due to dipole interactions between chains.¹³ In 1989, the work of Gatteschi et al. indicated dipole-based ordering near 8 K for the $\text{Mn}^{\text{II}}(\text{hfac})_2\text{NITR}$ (hfac = hexafluoroacetylacetonate; NITR = 2-*R*-4,4,5,5-tetramethyl-4,5-dihydro-1*H*-imidazolyl-1-oxy-3-oxide) magnets.¹⁴ The microscopic alignment of spins for most other magnets¹⁵ is controlled by a quantum-mechanical process termed exchange due to antisymmetrization of wave functions that comprise the overlap on bonds between spin sites. Hence, in contrast to the classical "through-space" dipolar interactions, the quantum-mechanical exchange is a "through-bond" effect.

Spin-orbit coupling results from an effective field due to electron interaction with its nucleus. In either a crystal or an isolated molecule the electrostatic fields of the neighboring atoms alter the charge cloud of the electron. If the symmetry of the surrounding atoms is sufficiently low (less than cubic), single-ion anisotropy (SIA) results, which establishes an energetically favorable direction for the spin. The SIA can therefore play

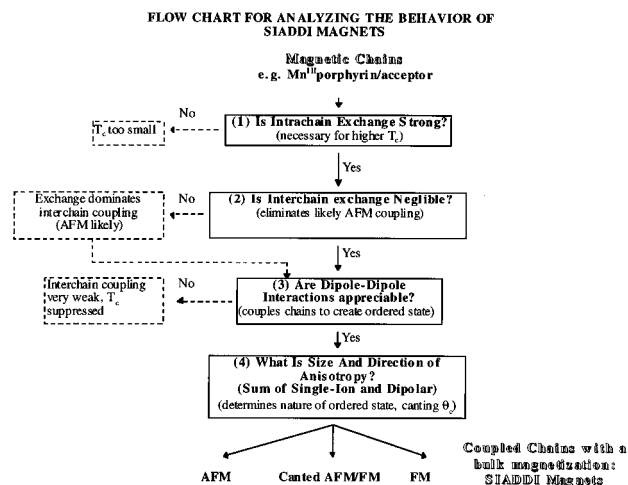


Figure 1. Flow chart for analyzing the magnetic behavior of SIADDI magnets.

a central role in determining the cant angle of a spin array. It also is responsible for the spectroscopically observed zero-field splittings.

We report here a novel mechanism for magnetic ordering based on weak dipole-dipole interactions together with modest SIA to couple magnetic chains leading to canted magnetic ordering at relatively high transition temperatures. We also report here examples of the presence of this mechanism in the family of $[\text{Mn}^{\text{III}}\text{porphyrin}]^+[\text{cyanocarbon}]^-$ magnets. By adding bulky substituent groups to the porphyrin to minimize exchange paths, advantage can be taken of the dipolar interactions leading to magnetic ordering. These side groups also alter the tilt angle for the porphyrin core with respect to the chain axis, thereby establishing the orientation and modifying the strength of the SIA.¹⁶ Together the SIA and dipolar interactions can lead to canted AFMs with net magnetic moments. The overall strategy has been outlined in the flow diagram shown in Figure 1. Antiferromagnetic exchange coupling within a chain of alternating spins of different magnitudes leads to ferrimagnetic chains. Instead of exchange, which is usually AFM,¹⁷ coupling the chains, minimization of the interchain exchange to the point of being negligible leads to the interchain coupling being dominated by magnetic dipole-dipole interactions. Thus, *by taking the counterintuitive approach of minimizing the most common (but usually AFM) interchain coupling mechanism (the quantum-mechanical process termed exchange) and relying upon a significantly weaker (but potentially FM) mechanisms, the classical through-space dipole-dipole interaction together with a modest onsite SIA, canted magnets with sizable T_c 's can be achieved. The single-ion anisotropy/dipole-dipole interaction (SIADDI) mechanism is expected to be a general mechanism for stabilizing canted magnets comprised of parallel linear chains.*

Model for Controlling the Magnetic Interactions

Essential to the construction of a system with a macroscopic (or bulk) magnetization is the manipulation

(7) Caneschi, A.; Gatteschi, D.; Sessoli, R.; Rey, P. *Acc. Chem. Res.* **1989**, *22*, 392. Pei, Y.; Kahn, O.; Sletten, J. *J. Am. Chem. Soc.* **1986**, *108*, 3143. Pei, Y.; Verdager, M.; Kahn, O.; Sletten, J.; Renard, J. P. *Inorg. Chem.* **1987**, *26*, 138.

(8) Kahn, O. *Adv. Inorg. Chem.* **1995**, *43*, 179. Kahn, O.; Pei, Y.; Nakatani, K.; Journaux, Y. *New J. Chem.* **1992**, *16*, 269. Kahn, O. *Struct. Bonding* **1987**, *68*, 89. Okawa, H.; Matsumoto, N.; Tamaki, H.; Ohba, M. *Mol. Cryst. Liq. Cryst.* **1993**, *233*, 257.

(9) Inoue, K.; Hayamizu, T.; Iwamura, H., *J. Am. Chem. Soc.* **1994**, *116*, 3173.

(10) For example: Ashcroft, N. W.; Mermin, N. D. *Solid State Physics*; W. B. Saunders Co.: London, 1976; p 673. Kittel, C. *Introduction to Solid State Physics*; John Wiley and Sons: New York, 1986; p 423.

(11) Reviews of some of the extensive studies of rare-earth-based compounds can be found in: Orton, J. W. *Electron Paramagnetic Resonance*; Iliffe: London, 1968. Cotton, S. A.; Hart, F. A. *The Heavy Transition Elements*; Wiley and Sons: New York, 1975. Carlin, R. L. *Magnetochemistry*; Springer-Verlag: New York, 1986; Chapter 9.

(12) Ehnholm, G. J.; Katila, T. E.; Lounasmaa, O. V.; Reivari P.; Kalvius G. M.; Shenoy, G. K. *Z. Physik* **1970**, *235*, 289.

(13) Dingle, R.; Lines, M. E.; Holt, S. L. *Phys. Rev.* **1969**, *187*, 643.

(14) Caneschi, A.; Gatteschi, D.; Renard, J. P.; Rey, P.; Sessoli, R. *Inorg. Chem.* **1989**, *28*, 3314. Caneschi, A.; Gatteschi, D.; Renard, J. P.; Rey, P.; Sessoli, R. *Inorg. Chem.* **1989**, *28*, 1976.

(15) In addition to the examples mentioned in the text, M. Drillon is currently studying a family of layered magnets proposed to order due to dipole interactions as reported at the Fifth International Conference on Molecule-Based Magnetism, Osaka, Japan, July 1996.

(16) The SIA of the Mn^{III} compounds contrasts with the small and usually ignored SIA of Mn^{II} compounds.

(17) Kahn, O.; Pei, Y.; Verdager, M.; Renard, J. P.; Sletten, J. *J. Am. Chem. Soc.* **1988**, *110*, 782.

of the interactions among the microscopic units (or spins) comprising the system. The exchange interactions can be described by the well-known spin Hamiltonian

$$H = -2J\vec{S}_1 \cdot \vec{S}_2 \quad (1)$$

where S_1 and S_2 are neighboring spins on sites "1" and "2". Here J represents the total interaction between these two spins. The sign of J (\pm) determines whether the spins will couple FM (+) or AFM (-). Even though strictly speaking the dipole-dipole interactions cannot be labeled as exchange (as noted above, exchange is a quantum-mechanical effect while dipole-dipole interactions are classical), it is useful to present them in an effective exchange form in order to compare the relative energies of the different interactions. Therefore, we divide the total J , J^{total} , into J^{exchange} and J^{dipole} such that

$$J^{\text{total}} = J^{\text{exchange}} + J^{\text{dipole}} \quad (2)$$

J^{exchange} is determined by the sum of several through-bond couplings including that due to orthogonality of orbitals (also known as potential exchange) and contributions that can be described by configuration interaction, including the kinetic exchange, spin polarization, and correlation exchange.¹⁸ The potential (or direct) exchange, which is always FM, is an intermolecular expression of Hund's rule. It can be accounted for by Hartree-Fock calculations and is maximized when the neighboring wave functions are orthogonal in the same spatial region. The next three terms in the sum can be described using second-order configuration interaction. The sign of the kinetic exchange will vary with the degeneracy of the sites and direction of charge transfer;¹⁹ it is usually greater in magnitude than the potential exchange. The kinetic exchange is related to the virtual transfer of an electron between spin centers and increases as the overlap of wave functions increases. Spin polarization also may be either FM or AFM depending on the nature of the exchange path. These are all short-range processes that vanish extremely rapidly with increasing separation between spin centers, J varying approximately²⁰ as $\sim r^{-n}$ (for example, n has been determined by some²¹ to be 12 in the XMF_3 and X_2MF_4 compounds). The creation of FM coupling by relying solely upon J^{exchange} thus requires the delicate balance of many factors, some of which have not been mentioned here.

In contrast, dipole-dipole interactions are long range (see eq 3) and will, in general, favor a FM state for dipole pairs that are free to rotate, i.e., SIA = 0. However, they usually are considerably weaker than J^{exchange} , and for that reason are almost always ignored. To compare J^{exchange} and J^{dipole} , we bring the dipole-dipole interaction energy, U , to an effective exchange form similar to eq 1 using the point-dipole approximation:

$$U = (g_1 g_2 \mu_B^2 / r^3) [\vec{S}_1 \cdot \vec{S}_2 - 3(\vec{S}_1 \cdot \vec{r})(\vec{S}_2 \cdot \vec{r}) / r^2] \quad (3)$$

where \vec{r} is the vector connecting spins S_1 and S_2 , g_1 and g_2 are the respective Landé g factors, and μ_B the Bohr magneton. Note the long-range r^{-3} dependence as opposed to the short-range exchange. We make the approximation that both spins lie either parallel or perpendicular to \vec{r} such that U is now proportional to $(g_1 g_2 \mu_B^2 / r^3)(S_1 S_2)$, with proportionality constant α . Comparing this to eq 1, we approximate

$$J^{\text{dipole}} = (\alpha/2) g_1 g_2 \mu_B^2 / r^3 \quad (4)$$

where α is a constant whose magnitude depends on the orientations of the spins and whose sign is fixed so as to be consistent with eq 1, i.e., antiparallel spins (-) and parallel spins (+). Calculations reported later in this work reveal a small but important magnitude for J^{dipole} .

An in-registry chain-structured material requires FM coupling between chains to have a spontaneous moment. Antiferromagnetic coupling between adjacent in-registry chains leads to the absence of a bulk moment. The strategy described herein is based upon (a) strong exchange-dominated coupling of spins within chains leading to ferrimagnetic or ferromagnetic chains (step 1 of Figure 1) and (b) dipolar-dominated coupling between chains leading to magnetic ordering. To achieve dipolar-dominated coupling between chains the small FM J^{dipole} must be greater than AFM J^{exchange} . Hence minimization of the interchain exchange and maximization of the interchain dipole interactions (steps 2 and 3 in Figure 1) can lead to a 3D magnet whose magnetic structure (AFM, canted AFM, FM) depends upon the SIA.

For simplicity we assume an orthorhombic unit cell with the chains parallel to one of the axes. Using second-order Green's function theory, the ordering temperature, T_c (at which a bulk moment appears if the system is FM) and the intra- and interchain exchange strengths can be related through²²

$$T_c = \sqrt{8} S(S+1) \sqrt{|J_{\text{intra}}| (|J_{1,\text{inter}}| + |J_{2,\text{inter}}|)} \quad (5)$$

where S is the magnitude of the spins being coupled and $J_{1,\text{inter}}$ and $J_{2,\text{inter}}$ are the interchain exchange strengths along the two directions perpendicular to the chain axis. Thus, to achieve a high T_c for chain compounds, it is necessary for the J_{intra} to be large to compensate for the small J_{inter} 's.

The ordered state of a system composed of chains coupled only by dipole-dipole interactions (i.e., SIA = 0) should be anisotropic, i.e., the spins will align along certain directions. If SIA also is present, these directions will be determined by the sum of the SIA imposed by the ligand field surrounding the metal ions and the dipolar anisotropy, step 5 of Figure 1. Hence in contrast to the spins being antiparallel within each chain, between chains the spins, as a consequence of the anisotropies, are likely to be neither completely parallel nor antiparallel but canted at some angle relative to one another. The following antisymmetric addition to the standard exchange Hamiltonian was developed phe-

(18) (a) Sinha, K.; Kumar, N. *Interactions in Magnetically Ordered Solids*; Oxford University Press: Oxford, 1980. Anderson, P. W. *Solid State Phys.* **1963**, *14*, 99. (b) Miller, J. S.; Epstein, A. J. *Angew. Chem., Int. Ed. Engl.* **1994**, *33*, 385.

(19) Miller, J. S.; Epstein, A. J. *J. Am. Chem. Soc.* **1987**, *109*, 3850.

(20) $n \sim 10$ in the following studies: Bloch, D. *J. Phys. Chem. Solids* **1963**, *27*, 881. Lowndes, D. H.; Finegold, L.; Rogers, R. N.; Morosin, B. *Phys. Rev.* **1969**, *186*, 515.

(21) de Jongh, L. J.; Block, R. *Physica* **1975**, *79B*, 568.

(22) Richards, P. M. *Phys. Rev. B* **1974**, *10*, 4687.

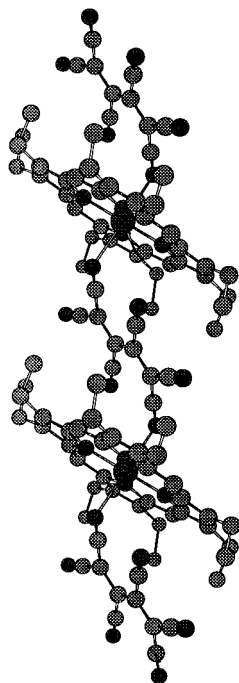


Figure 2. Segment of the chain structure of [MnOEP][HCBd]. For clarity, H atoms are not shown.

nomenclologically by Dzialoshinski and Moriya²³ to describe canted systems:

$$H_{\text{DM}} = \vec{d} \cdot \vec{S}_1 \times \vec{S}_2 \quad (6)$$

in which the coupling constant d can be approximated as

$$|d| \approx (2\Delta g/g)J \quad (7)$$

where $\Delta g = g - 2$.

Figure 1 schematically summarizes the process for achieving bulk magnetization using magnetic chains, interchain dipole–dipole interactions, and SIA. Step 1 alerts to the need for large intrachain exchange to achieve high T_c . The necessity of elimination of interchain exchange is pointed out in step 2. Obtaining sizable dipole–dipole interactions is brought out in step 3. Finally, the key roles of single-ion and dipolar anisotropy are emphasized in step 4. It is pointed out that disorder, if present, will alter the final magnetic state.

Application of Model to the Mn^{III}Porphyrim/Acceptor Family of Quasi-1D Magnets

The family of linear chain metalloporphyrin electron-transfer salts exhibit a variety of magnetic behaviors that can be explained by this general SIADDI model. These compounds consist of parallel $\cdots D^+ A^- D^+ A^- \cdots$ chains ($D^+ = \text{Mn}^{\text{III}}$ porphyrin cations with spin $S_1 = 2$ and $A^- = \text{trans-}\mu_2\text{-bonded anions, such as [TCNE]}^- \text{ or [HCBd]}^-$ (HCBd = hexacyanobutadiene) with spin $S_2 = 1/2$), as exemplified by [MnOEP][HCBd] (OEP = octaethylporphyrinato, Figure 2). The 1D structural nature of these magnets is due to the covalent bonding of the two spin-carrying units, $S_1 = 2$ and $S_2 = 1/2$, along the chain axis, and the absence of covalent bonding

perpendicular to it. While this paper focuses on the properties of three members of the family ([Mn^{III}OEP][HCBd], [Mn^{III}TPP][TCNE]· x o-DCB ($0 \leq x \leq 3$) and [Mn^{III}TPP][TCNE]· x o-Xy; ($0 \leq x \leq 3$) o-DCB = *o*-dichlorobenzene and o-Xy = *o*-xylene are solvents of crystallization; TPP = *meso*-tetraphenylporphyrinato),²⁴ it should be noted that the ideas presented herein are applicable to all members (more than 20) of this porphyrin chain family²⁵ for which the ferrimagnetic chain is intact. Small changes in the [Mn^{III}porphyrin]⁺ alter the weak interchain exchange pathways while maintaining the strong linear chain ferrimagnetic nature. When the AFM interchain exchange is negligible as compared to the FM dipole–dipole interactions, the latter together with the SIA, will dominate potentially leading to magnetic ordering with a net moment.

We have begun a systematic study of the dependence of the intrachain exchange strength on various parameters, such as bond angle, bond distance, and acceptor, in order to maximize this exchange (step 1 in Figure 1). From the close approach of the anion to the Mn^{III} and the absence of orthogonality of the spin-containing orbitals, the relatively strong intrachain magnetic coupling of the compounds is expected to be kinetic exchange. The intrachain exchange can be determined by examining the temperature, T , dependence of the magnetic susceptibility, χ , and fitting it to theoretical predictions describing chains of alternating spins. An applicable model is that of Seiden²⁶ for an isolated alternating classical/quantum spin chain, assuming that the $S_1 = 2$ [MnOEP]⁺ behaves classically and the $S_2 = 1/2$ [HCBd][−] behaves quantum mechanically. The prediction for the product of the magnetic susceptibility and temperature, χT , as a function of temperature allows three free parameters: the intrachain exchange, J_{intra} , and the Landé g factors of both spins, g_{S_1} and g_{S_2} .

Figure 3a displays $\chi_{\text{DC}} T$ versus T for [MnOEP][HCBd] along with a best fit to the data. The static susceptibility χ_{DC} (defined as M/H , where M is the magnetization of a powdered sample and H the applied field) was measured using a Quantum Design SQUID magnetometer operating at $H = 1$ T. The g factor of the acceptor (g_{S_2}) was fixed at its expected value of 2.00.²⁷ A best fit to the Seiden model was obtained using a least-squares fitting algorithm and $J_{\text{intra}} = -172 \pm 3$ K and $g_{S_1} = 1.92 \pm 0.04$, a reasonable value for the $3d^4$ electronic configuration of the Mn^{III}porphyrin ion.²⁸ Due to the large J_{intra} , the minimum in χT , characteristic of ferrimagnets, should occur above 350 K. Similar fits have been made for other compounds in the family²⁹ including the two discussed in this paper: [MnTPP][TCNE]· x o-DCB ($J_{\text{intra}} = -140 \pm 3$ K, Figure 3b) and

(24) The magnetic data reported here for the [Mn^{III}TPP][TCNE]· x o-DCB compound is consistent with $x = 2$, while that for the [Mn^{III}TPP][TCNE]· x o-Xy compound is consistent with $x = 1$.

(25) Miller, J. S.; Vazquez, C.; Jones, N. L.; McLean, R. S.; Epstein, A. J. *J. Mater. Chem.* **1995**, *5*, 707. Miller, J. S.; Calabrese, J. C.; McLean, R. S.; Epstein, A. J. *Adv. Mater.* **1992**, *4*, 498. Bohm, A.; Vazquez, C.; McLean, R. S.; Calabrese, J. C.; Kalm, S. E.; Manson, J. L.; Epstein, A. J.; Miller, J. S. *Inorg. Chem.* **1996**, *35*, 3083.

(26) Seiden, J. *J. Phys. (Paris) Lett.* **1983**, *44*, L-947.

(27) Phillips, W. D.; Rowell, J. C.; Weismann, S. I., *J. Chem. Phys.* **1960**, *33*, 28. Bencini, A.; Gatteschi, D. *EPR of Exchange-Coupled Systems*; Springer-Verlag: Berlin, 1990.

(28) Kennedy, B. J.; Murray, K. S. *Inorg. Chem.* **1985**, *24*, 1557. Abragam, A.; Bleaney, B. *Electron Paramagnetic Resonance of Transition Ions*; Dover: 1986, Chapter 7.

(29) Wynn, C. M.; Girtu, M. A.; Epstein, A. J.; Miller, J. S.; Sugiura, K.-I., in preparation.

(23) Moriya, T. In *Magnetism*; Rado, G. T., Suhl H., Eds.; Academic Press: New York, 1963; Vol. 1, p 86.

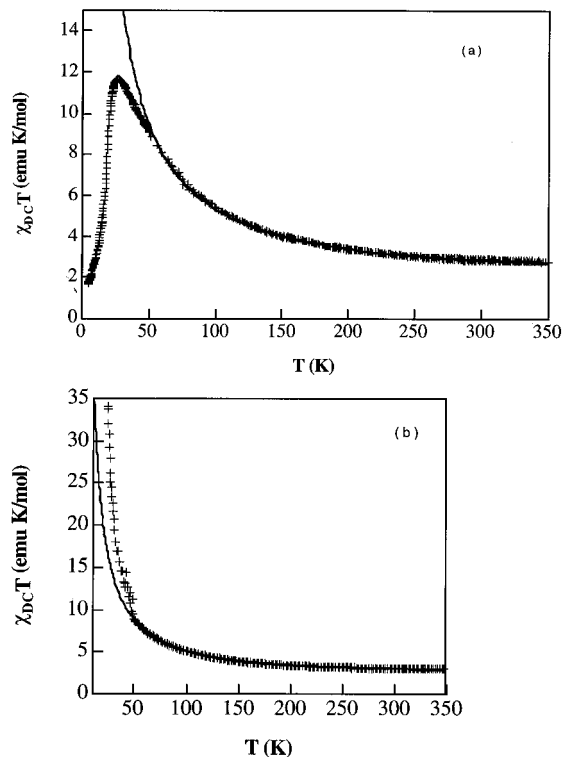


Figure 3. The product of the magnetic susceptibility and temperature $\chi_{DC}T$ as a function of temperature T for (a) [MnOEP][HCBD] and (b) [MnTPP][TCNE]· xO -DCB. Data were recorded in a magnetic field of 1 T. Lines are fits to the predictions for alternating quantum/classical spin ferrimagnetic chains.

[MnTPP][TCNE]· xO - Xy ($J_{intra} = -83 \pm 2$ K).

The low-temperature deviations of the χT product from the isolated chain (1D) predictions (Figure 3) are attributed to the effects of interchain magnetic interactions. Below 50 K, the χT product increases more rapidly than the 1D predictions for the TPP-based compounds, indicating FM coupling of the chains, whereas in the OEP-based compound χT falls below the 1D predictions, indicating AFM coupling of the chains. We correlate these magnetic differences with differences in the interchain $J_{inter}^{exchange}$, showing that it is negligible for the TPP family but not for the [MnOEP][HCBD].

To calculate $J_{inter}^{exchange}$, the distribution of spin on the repeat unit and between the chains must be known. Polarized neutron diffraction has shown the spin of [TCNE] $^-$ is delocalized with a significant fraction (0.10 μ_B) at each nitrogen site.³⁰ The spin on the [HCBD] $^-$ also is delocalized.³¹ On the basis of an NMR analysis of the spin density of Mn^{III}TPPCl, the spin on the $S_1 = 2$ Mn^{III}porphyrin is expected to be mostly localized on the Mn^{III}, with 0.09 μ_B per nitrogen atom and less than 0.02 μ_B on each of the pyrrol carbons.³²

The interchain exchange paths change as the porphyrin is altered from OEP to TPP (Figure 4). The strongest exchange pathways are those involving a direct overlap of spin-carrying orbitals. For simplicity, we treat the spin as if it were confined to the Mn^{III}-

porphyrin unit, excluding the substituent phenyl or ethyl groups.³³ The closest and most important interchain pathway for [MnOEP][HCBD] is displayed in Figure 4a. Porphyrins on adjacent chains are parallel to each other and overlapping at the edges, with a perpendicular separation of only 3.47 Å, allowing overlap, albeit weak, of the partially occupied π molecular orbitals. Such an overlap does not occur in any of the TPP-based compounds studied to date. This is due to the larger phenyl groups and much larger porphyrin–porphyrin distances (well in excess of the sum of van der Waals radii). In the absence of direct porphyrin–porphyrin overlap in the TPP family, interaction mediated via the phenyls (Figure 4b) will determine the exchange.

An estimate of the interchain exchange in the [MnOEP][HCBD] is made by referring to work on similar systems discussing the exchange due to the overlap of neighboring π orbitals such as the dianion of the benzene dimer, phenyl carbene clusters, and nitroxide pairs with parallel interplane conformations. The [(C₆H₆)₂]²⁻ dimer consists of eclipsed benzene radical anions separated by a distance d . Bagus and Torrance³⁴ estimated the exchange in such a system as a function of d by using configuration interaction wave functions based on orbitals of the isolated radical anion. Their results show appreciable interactions even for distances greater than the sum of the van der Waals radii and estimate $J_{inter}^{exchange} \approx 10^3$ K at $d = 3.47$ Å (the separation of the parallel porphyrin planes in the [MnOEP][HCBD]). However, this is an overestimate as the [MnOEP]⁺ planes are not eclipsed as in [(C₆H₆)₂]²⁻. To account for the overlap reduction due to the slippage, the results of Yamaguchi et al.³⁵ on phenyl carbene clusters are used. Using unrestricted Hartree–Fock calculations, they show that if one of the benzene rings is shifted relative to the other such that only two carbons are eclipsing one another, the exchange strength is reduced by less than an order of magnitude. Assuming that the porphyrin–porphyrin system corresponds to a worst-case scenario in which the exchange is maximally reduced, we estimate that the exchange will be reduced by a factor of 10 to 10² K. The ramification of carbons being noneclipsed has been addressed by Yamaguchi and co-workers in their work on phenyl carbenes and also nitroxide pairs.³⁶ As the molecules are shifted relative to one another, the dominant exchange mechanism varies (i.e., spin polarization as opposed to kinetic or potential exchange). Such shifting can be estimated to reduce the exchange in our system (for which only 3 of 25 C's are almost eclipsed) by another order of magnitude to 10 K. Last, we address the effect of the reduced spin density on the porphyrin carbons. The spin density on a carbon of a [C₆H₆] $^-$ will be approximately 0.17 μ_B , an order of magnitude greater than the density of the porphyrin carbon.³² Since the exchange is related to the square of the spin density, a further reduction by 2 orders of magnitude to 0.1 K is expected. Thus the exchange can be estimated at 0.1

(30) Zheludev, A.; Grand, A.; Ressouche, E.; Schweizer, J.; Morin, B. G.; Epstein, A. J.; Dixon, D. A.; Miller, J. S. *Angew. Chem., Int. Ed. Engl.* **1994**, *33*, 1397.

(31) Sugiura, K.-I.; Arif, A. M.; Rittenberg, D.; Schweizer, J.; Ohlstrom, L.; Epstein, A. J.; Miller, J. S. *Chem. Eur. J.* **1997**, *3*, 000.

(32) Mun, S. K.; Mallick, M. K.; Mishra, Sh.; Chang, J. C.; Das, T. P. *J. Am. Chem. Soc.* **1981**, *103*, 5024.

(33) The same conclusions can be reached by treating the entire entity (porphyrin core and substituent) as the ground state, with kinetic exchange between these larger units.

(34) Bagus, P. S.; Torrance, J. B. *Phys. Rev. B* **1989**, *39*, 7301.

(35) Yamaguchi, K.; Toyoda, Y.; Fueno, T. *Chem. Phys. Lett.* **1989**, *159*, 459.

(36) Kawakami, T.; Yamanaka, S.; Mori, W.; Yamaguchi, K.; Kajiwara, A.; Kamachi, M. *Chem. Phys. Lett.* **1995**, *235*, 414.

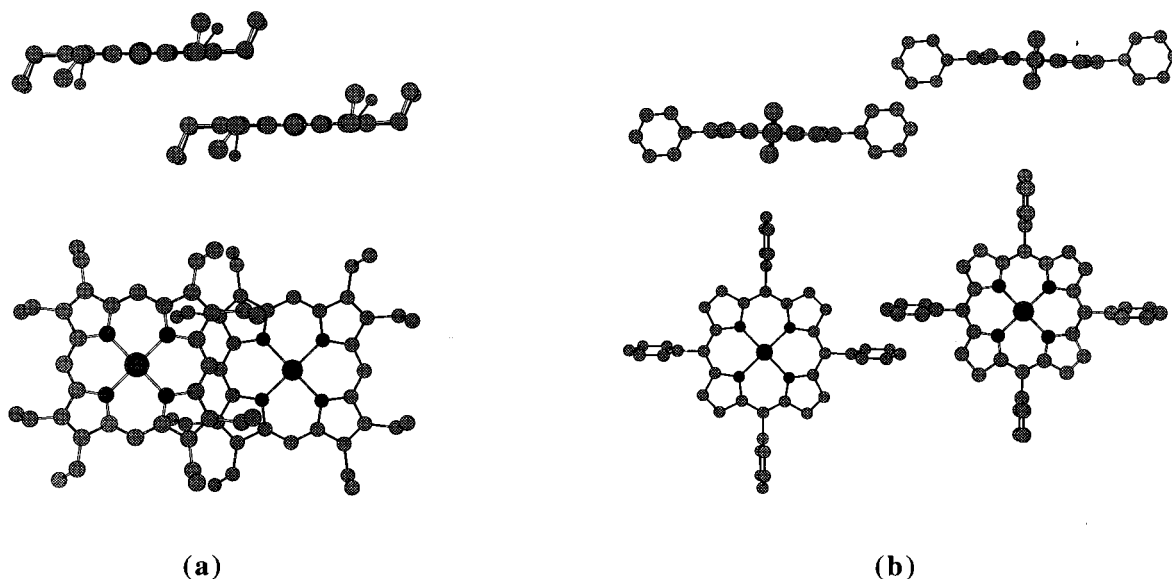


Figure 4. Interchain exchange pathways for (a) [MnOEP][HCBd] and (b) [MnTPP][TCNE]·*o*-Xy. For clarity, H atoms are not shown.

K. Although small, it is still an order of magnitude larger than the dipole–dipole energy.

The absence of direct interchain overlap coupled with larger interchain separations in the TPP-based compounds implies a significantly weaker interchain exchange relative to [MnOEP][HCBd]. The van der Waals distance (3.5 Å) is significantly less than even the shortest phenyl–phenyl distance in any of the TPP members (3.75 Å in the [MnTPP][TCNE]·*o*-Xy, Figure 4b). As the interchain exchange decreases rapidly with increasing separation, it is expected to be drastically reduced.³⁷ On the basis of these factors we conclude that the interchain exchange in the TPP-based compounds is negligible.

$\mathcal{J}^{\text{dipole}}$ is estimated using eq 4. A planar configuration is assumed (spins on neighboring chains in registry with one another) in which each primary chain (parallel to the *z*-axis) has four parallel nearest-neighbor chains offset from the central chain in the *x*, $-x$ and *y*, $-y$ directions (see Figure 5). Since these interchain separations are not the same in length, two interchain $\mathcal{J}^{\text{dipole}}$ values are calculated. The stronger effective exchange, $\mathcal{J}_{1,\text{inter}}^{\text{dipole}}$ (arising from the shorter interchain distance) is calculated assuming the spin 2–spin 2 interaction between neighboring chains (being a factor of 16 greater than the spin $1/2$ –spin $1/2$ interaction) dominates, forcing the neighboring spin 2's to lie parallel (FM) to one another and along \vec{r} , the vector connecting the two chains. Comparing eqs 3 and 4 for two nearest neighbors along this axis yields $\alpha = +4$. The sign has been assigned positive as the spins are parallel. We calculate the weaker effective exchange, $\mathcal{J}_{2,\text{inter}}^{\text{dipole}}$, by again assuming the spin 2–spin 2 interaction dominates, but noting that the previous (stronger) interchain interaction has already fixed the direction of the primary spin to be along the axis connecting it to the closer neighbor chain.

(37) Further, the phenyl rings are twisted nearly out of conjugation with the porphyrin plane (angles typically greater than 75°), significantly reducing the phenyl–porphyrin overlap, and hence nearly eliminating spin delocalization from the porphyrin to the covalently bonded phenyl ring. In addition, the π and π^* energy levels of the porphyrin and the covalently bonded phenyls are mismatched, further inhibiting delocalization of spin.

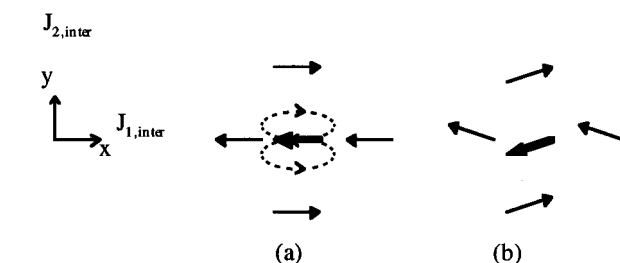


Figure 5. Schematic top view of the spins of model ferrimagnetic chains showing the primary spin (bold) along with its four nearest neighbors. (a) Depicts the approximation used to calculate the effective dipolar exchanges ($\mathcal{J}_{1,\text{inter}}$ and $\mathcal{J}_{2,\text{inter}}$). It also shows the dipole field of the primary spin (dashed lines). (b) Depicts a more realistic, canted, configuration for the spins. Note that the spins may have components out of the plane of the page.

Thus the spins on the primary chain are fixed perpendicular to the axis between the primary chain and the further chain. In this scenario, the most favorable position for the farther spin 2 is to lie antiparallel to the primary spin 2. Two nearest neighbors along this axis yields $\alpha = -2$ (the negative sign is assigned because the spins are antiparallel). Thus, in this configuration the primary chain aligns FM with its neighbors in one (closer) direction and then AFM with its neighbors along the other (farther) direction. Using these assumptions and the reported lattice parameters, the effective $\mathcal{J}^{\text{dipole}}$ values ($\mathcal{J}_{1,\text{inter}}^{\text{dipole}}$ and $\mathcal{J}_{2,\text{inter}}^{\text{dipole}}$) in the two directions perpendicular to the chain axis have been calculated (Table 1). If $|\mathcal{J}_{2,\text{inter}}^{\text{dipole}}| \ll |\mathcal{J}_{1,\text{inter}}^{\text{dipole}}|$ as assumed in Figure 5a, the resulting system is AFM. However, as $|\mathcal{J}_{2,\text{inter}}^{\text{dipole}}|$ is increased relative to $|\mathcal{J}_{1,\text{inter}}^{\text{dipole}}|$, canting of the spins will occur, resulting in a net magnetic moment (referred to as a canted or weak ferromagnet). The presence of the Mn^{III} single-ion anisotropy (SIA) will alter this cant angle.

Discussion: SIA/Dipole–Dipole Interaction Based Magnets

The weakly interchain coupled [MnOEP][HCBd] and [MnTPP][TCNE]·solvent (solvent is *xo*-DCB, *xo*-Xy)

Table 1. Intrachain (from Seiden Model Fit to Experimental Data) and Interchain (from Lattice Parameters and Point-Dipole Approximation) Exchange Parameters for Four Members of the Porphyrin Family, along with the Theoretical and Experimental Values for T_c

compound	J_{intra} (K)	d_1 (Å)	d_2 (Å)	$J_{1,\text{inter}}^{\text{dipole}}$ (mK)	$J_{2,\text{inter}}^{\text{dipole}}$ (mK)	$J_{1,\text{inter}}^{\text{dipole}}$ (K)	$J_{2,\text{inter}}^{\text{dipole}}$ (K)	T_c^{dipole} (K) (theory)	T_c (K) (expt)
[MnOEP][HCBD]	-172	8.02	12.33	9.7	-1.3	~ -0.1	0	14	8
[MnTPP][TCNE]· <i>o</i> Xy	-83	9.26	13.29	6.3	-1.0	0	0	8	8
[MnTPP][TCNE]· <i>xo</i> DCB	-140	12.87	12.89	2.3	-1.2	0	0	8	10
[MnTPP][TCNE]·2PhMe ^a	~ -115	11.01	12.50	3.7	-1.3	0	0	8	13

^a A detailed discussion [MnTPP][TCNE]·2PhMe has been reported elsewhere (see reference in text).

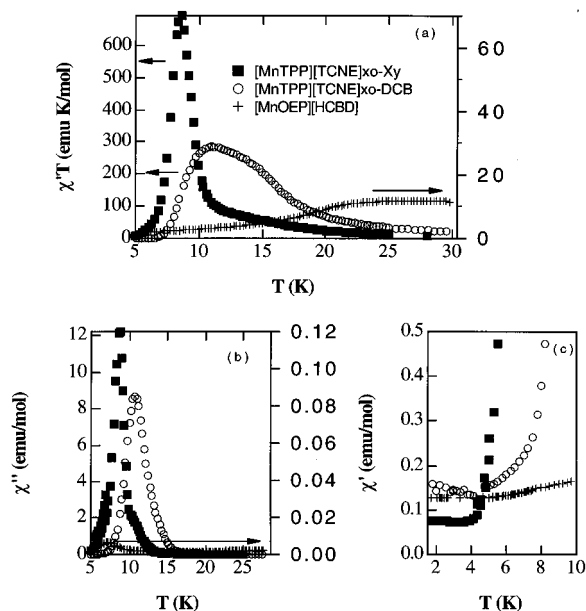


Figure 6. Low temperature ac magnetic data for powdered [MnOEP][HCBD] (pulses), [MnTPP][TCNE]·*xo*-Xy (squares), and [MnTPP][TCNE]·*xo*-DCB (circles). All data were recorded in zero dc field and 1 Oe ac field at a frequency of 1 KHz. (a) The product of the in-phase ac susceptibility and temperature, $\chi' T$ as a function of temperature T . The [MnOEP][HCBD] data are plotted using the right-hand axis. (b) The out-of-phase ac susceptibility, χ'' as a function of T . The [MnOEP][HCBD] data are plotted using the right-hand axis. (c) The in-phase ac susceptibility, χ' as a function of T .

compounds enable a test of the concept of a SIA/dipole-dipole interaction based magnet. The intrachain exchange values, obtained by fits to the Seiden 1D model, together with the calculations for $J_{\text{inter}}^{\text{exchange}}$ and $J_{\text{inter}}^{\text{dipole}}$ obtained with the algorithms of the previous section are summarized in Table 1. Only for [MnOEP][HCBD] is the $J_{\text{inter}}^{\text{exchange}}$, which is AFM, appreciable as compared with $J_{\text{inter}}^{\text{dipole}}$. As seen in Figure 3, the interchain interactions are FM for the TPP-based compounds (the product of the experimental susceptibility, χ_{exp} , and T , $\chi_{\text{exp}} T$, is greater than the predicted $\chi_{1D} T$ at low temperatures) indicating that $J_{\text{inter}}^{\text{dipole}}$ is FM in these compounds, while the interchain interactions are AFM for the [MnOEP][HCBD] ($\chi_{\text{exp}} T < \chi_{1D} T$ at low temperatures). Figure 6a, in which the $\chi' T$ product (related to the effective strength of a magnet) for the TPP-based members is 2 orders of magnitude greater than the [MnOEP][HCBD], highlights the dramatic effects of an elimination of the interchain exchange. Here χ' and χ'' refer to the in- and out-of-phase ac susceptibilities, respectively.

A transition to long-range order with a spontaneous moment is marked by the appearance of a nonzero χ'' , along with a peak in χ' , (Figure 6b). Using these

criteria, the T_c 's of the TPP-based compounds were estimated as the maximum in $\chi''(T)$ (Table 1). Calculating T_c for the [MnOEP][HCBD] using estimates of J_{inter} and J_{intra} is complicated by two factors: the existence of an AFM exchange competing with a FM dipole-dipole interaction, and the significant difference in average interchain distance along the two crystallographic directions between parallel chains (8.02, 12.33 Å). These factors combine to create multiple magnetic transitions to states with different lattice dimensionalities.³⁸ Because of the absence of χ'' indicative of an AFM transition³⁹ we attribute the transition near 20 K to AFM exchange, while the 8 K transition exhibits χ'' and is attributed to the FM dipole-dipole interactions.

The observed T_c 's compare favorably with those determined by the combination of eq 5 with the estimated values of $J_{\text{inter}}^{\text{dipole}}$. To use eq 5 to obtain a T_c (Table 1), we assumed that $S = 3/2$ due to a strong AFM coupling between the $S_1 = 2$ and the $S_2 = 1/2$. Also included in Table 1 are data for [MnTPP][TCNE]·2PhMe.⁴⁰ The results for [MnOEP][HCBD] are treated with caution because of the expected effects of the competition between the $J_{\text{inter}}^{\text{dipole}}$ and $J_{\text{inter}}^{\text{exchange}}$, which should weaken the dipolar effects. Note that including the estimated $J_{\text{inter}}^{\text{exchange}}$ of [MnOEP][HCBD] in eq 5 leads to an even larger T_c than displayed in Table 1. The approximate agreement between this analysis and the experiment shown in Table 1 provides strong evidence that the porphyrin family is indeed a family of "dipole-dipole" based magnets. However, in these compounds the SIA is responsible for the pattern of 3D ordering.

Differences among members of this family without interchain exchange, e.g., [MnTPP][TCNE]·*xo*-Xy and [MnTPP][TCNE]·*xo*-DCB (note the differences in low-temperature χT products despite similar T_c 's), demonstrate the importance of the final step in the flow diagram (Figure 1). Assuming $J_{\text{inter}}^{\text{exchange}}$ is negligible, the sum of the two anisotropies in a system (single-ion and dipolar) determines whether the magnets are ferromagnets, antiferromagnets, or weak ferromagnets (WF). Weak ferromagnets are magnets in which the spin vectors cancel one another in one direction but leave an uncompensated component in a perpendicular direction. The canting angle, θ_c , between the neighbor spins determines the size of the uncompensated or WF moment and thus the strength of the magnet. Note θ_c

(38) Wynn, C. M.; Girtu, M. A.; Epstein, A. J.; Miller, J. S., in preparation.

(39) Palacio, F.; Lazaro F. J.; Van Duyneveldt, A. J. *Mol. Cryst. Liq. Cryst.* **1989**, *176*, 289.

(40) Morin, B. M. Ph.D. Thesis, The Ohio State University, 1994. Brinckerhoff, W. B. Ph.D. Thesis, The Ohio State University, 1995. Brinckerhoff, W. B.; Morin, B. G.; Brandon, E. J.; Miller, J. S.; Epstein, A. J. *J. Appl. Phys.* **1996**, *79*, 6147.

= 180° corresponds to an AFM whereas $\theta_c = 0^\circ$ corresponds to a FM.

The Hamiltonian of eq 6, describing canted systems, can be used to derive an expression for the behavior of the powder susceptibility at low temperatures. The susceptibility at low temperatures is predicted to approach a constant with a value of⁴¹

$$\chi = g^2 d^2 / 24 J^3 \quad (8)$$

Combining eqs 7 and 8 yields

$$\chi = \Delta g^2 / 6 J \quad (9)$$

The low-temperature behavior of the compounds (Figure 6c) is in agreement with these predictions in that they all approach a constant value at low temperatures. Using $\Delta g = 0.08$ for [MnOEP][HCBD], a susceptibility within an order of magnitude of the experimentally observed value is obtained. As expected for a WF within our temperature range near T_c , the powder $\chi(T)$ cannot be fit to a power law divergence (scaling analysis).⁴²

The origin of the spin cant angle is of importance. It is determined by several factors including the relative strengths of the two interchain dipole–dipole “ J s”, i.e., $J_{1,inter}^{dipole} / J_{2,inter}^{dipole}$, the registry of neighboring chains and the SIA due to the ligand field at the Mn^{III}. As noted earlier, the latter is determined by the local symmetry about and the electronic structure of the Mn^{III} ion, and this SIA will establish its own preferred direction for the spin. The most energetically favorable situation for a system with both SIA and dipole–dipole anisotropy will be one in which the preferential spin direction is at an angle somewhere intermediate to the direction determined by the ligand field and that determined by the dipole–dipole interactions.

To determine the preferential spin direction the strength of the SIA energy relative to the dipole–dipole energy is important. The magnitude of the zero-field

splitting in the porphyrin compounds has been estimated to be about 1 K,⁴³ an order of magnitude greater than J^{dipole} , thus it is a significant factor in determining the cant angles. Its direction is determined by the angle between the N(of TCNE)–Mn–N(of TCNE) axis and the chain axis, and varies in the TPP family from 14.8° (*xo*-Xy) to 31.0° (*xo*-DCB). Note that while the SIA is very important in determining the nature of the ordered state (θ_c and resulting bulk moment if any) induced by the dipole–dipole interactions, it cannot by itself, being an on-site energy, lead to magnetic ordering.

In conclusion, we have presented a mechanism for achieving bulk canted magnetic ordering with substantial T_c 's via interchain classical dipole–dipole interactions and onsite SIA for linear chain magnets with weak interchain exchange. This contrasts with the near universal role of the quantum-mechanical process of exchange in stabilizing order in magnetic materials. Utilizing the Mn^{III}porphyrin/cyanocarbon acceptor family, we have demonstrated (1) the use of substituent groups keeps chains apart, thereby reducing the AFM exchange so dipole–dipole interactions dominate (2) the choice of porphyrin substituent and solvent changes the cant angle of the porphyrin, thereby changing the direction and affecting the magnitude of the SIA, thus affecting the final magnetic ordering pattern, (3) by incorporating increased intrachain exchange in one direction, sizable T_c 's can be obtained despite the small size of the dipole–dipole interactions between chains. We have developed a general scheme (Figure 1) for assessing the important parameters necessary for a SIADDI-stabilized bulk magnetic moment in magnetic chain compounds. It has not escaped our attention that the concept of SIADDI-based magnets is general and may apply to other classes of magnets, including metallocene-cyanocarbon electron-transfer salts.^{18b}

Acknowledgment. This work was supported in parts by the DOE under Grant DE-FG02-86BR45271 and DE-FG03-93ER45504 and by the NSF under Grant CHE9320478.

CM970256C

(41) Kahn, O. *Molecular Magnetism*; VCH: New York, 1993, p 140.
 (42) Groenendijk, H. A.; Van Duyneveldt, A. J. *Physica* **1982**, *115B*, 41.

(43) Dugad, L. B.; Behere, D. V.; Marathe, V. R.; Mitra, S. *Chem. Phys. Lett.* **1984**, *104*, 353. Behere, D. V.; Marathe V. R.; Mitra, S. *Chem. Phys. Lett.* **1981**, *81*, 57.